STRUCTURE OF LOW-SPIN STATES IN ^{45}Sc STUDIED VIA COULOMB EXCITATION*

M. Matejska-Minda[a,b], P.J. Napiorkowski[b], K. Sieja[c]
P. Bednarczyk[a], T. Abraham[b], A. Agarwal[d], I. Ahmed[e]
S. Bhattacharya[f], R.K. Bhowmik[d], D.T. Doherty[g], S. Dutt[h]
K. Hadyńska-Klęk[b], J. Iwanicki[b], A. Jhingan[e], J. Kaur[i]
M. Kicińska-Habior[j], M. Kisieliński[b], M. Komorowska[b]
M. Kowalczyk[b], M. Kumar[e], R. Kumar[e], S. Kumar[e], D. Kumar[k]
A. Maj[a], T. Marchlewski[b], P. Matuszczak[b], V. Nanal[l]
A. Nannini[m,n], M. Palacz[b], R. Palit[l], L. Próchniak[b]
N.K. Rai[o], M. Rocchini[m,n], M. Saxena[b,p], W. Satuła[j]
M. Shuaib[h], M. Siciliano[q,r], A. Sood[s], J. Srebrny[b]
A. Stolarz[b], J. Styczeń[a], T. Trivedi[t], A.K. Tyagi[o]
B. Wasilewska[a], H.J. Wollersheim[u], K. Wrzosek-Lipska[b]
M. Zielińska[v]

[a]Institute of Nuclear Physics Polish Academy of Sciences, Kraków, Poland
[b]Heavy Ion Laboratory, University of Warsaw, Poland
[c]University of Strasbourg, IPHC, Strasbourg, France
[d]Department of Physics, Bareilly College, India
[e]IUAC, New Delhi, India
[f]Department of Pure and Applied Physics, Guru Ghasidas University, India
[g]Department of Physics, University of Surrey, Guildford, UK
[h]Department of Physics, Aligarh Muslim University, India
[i]IFIN-HH, Bucharest-Măgurele, Romania
[j]Faculty of Physics, University of Warsaw, Poland
[k]Department of Physics, IIT, Roorkee, Uttarakhand, India
[l]Department of Nuclear and Atomic Physics, TIFR, Mumbai, India
[m]University of Florence, Italy
[n]INFN, Sezione di Firenze, Firenze, Italy
[o]Department of Physics, Banaras Hindu University, Varanasi, India
[p]University of Delhi, New Delhi, India
[q]INFN, LNL, Legnaro, Italy
[r]ANL, Argonne, USA
[s]Department of Physics, Indian Institute of Technology Ropar, Punjab, India
[t]Department of Physics, University of Allahabad, Prayagraj, India
[u]GSI, Darmstadt, Germany
[v]Irfu, CEA, University Paris-Saclay, Gif-sur-Yvette, France

Received 3 January 2024, accepted 8 February 2024,
published online 24 April 2024

The electromagnetic structure of ^{45}Sc at low excitation energy was investigated via low-energy Coulomb excitation at the Heavy Ion Laboratory (HIL) of the University of Warsaw and at the Inter-University Accelerator Centre (IUAC) in New Delhi. A set of reduced E2, E3, and M1 matrix elements was extracted from the collected data using the GOSIA code. The reduced transition probability $B(\mathrm{E2}; 11/2^- \rightarrow 7/2^-)$ has been determined, allowing us to deduce the lifetime of the $11/2^-$ state at 1237 keV. In addition, the upper limit on the reduced transition probability $B(\mathrm{E3}; 7/2^- \rightarrow 5/2^+)$ has been determined for the first time. New large-scale shell-model and beyond-mean-field calculations were performed to interpret the structure of this nucleus.

DOI:10.5506/APhysPolBSupp.17.3-A3

1. Introduction

Odd-mass nuclei in the lower part of the $f_{7/2}$ shell provide striking examples of non-closure effects of the $N = Z = 20$ shells, which result in the occurrence of many low-lying positive-parity "intruder" states, *e.g.* in ^{43}Sc, ^{45}Sc, ^{47}Sc, ^{45}Ti, ^{45}V, and ^{49}V [1–3]. The structure of odd-mass Sc isotopes is particularly interesting due to the coexistence of positive-parity and negative-parity bands near the ground state. For example, in ^{45}Sc the ground state is almost degenerate as the $3/2^+$ intruder state with a half-life $T_{1/2} = 318$ ms is only 12.4 keV above the energy of the $7/2^-$ level. The ^{45}Sc has one additional proton in the $f_{7/2}$ shell outside the magic ^{40}Ca core. The presence of the odd proton strongly impacts the core polarization, which is manifested by shape coexistence effects in this stable ^{45}Sc isotope [4]. In addition, a collinear laser spectroscopy experiment [5] showed the difference in the charge radii between the ground and isomeric states in this nucleus. The electric quadrupole moment for the isomeric state was found to have a positive sign and a value of $Q_s = +0.28(5)$ eb [5], in comparison with $Q_s = -0.22(1)$ eb for the ground state [6]. The positive-parity band built on the $3/2^+$ isomer can be seen as a proton hole in the $d_{3/2}$ orbital weakly coupled to the collective deformed ^{46}Ti core, while the negative-parity structure can be interpreted as a proton in the $f_{7/2}$ orbital coupled to the spherical ^{44}Ca core [4]. However, the large-scale shell-model approach, despite adopting a simple excitation mechanism for the $d_{3/2}$ proton, faces serious difficulties in achieving such low excitation energy. To unravel the nature of the ^{45}Sc nucleus, dedicated Coulomb-excitation experiments were conducted at HIL at the University of Warsaw and at IUAC in New Delhi, aiming to precisely measure the matrix elements of transitions in the vicinity of the $3/2^+$ isomer.

* Presented at the XXXVII Mazurian Lakes Conference on Physics, Piaski, Poland, 3–9 September, 2023.

2. Experimental details

A dedicated experiment to study the structure of ^{45}Sc at low excitation energy was performed at HIL, University of Warsaw. A ^{32}S beam of 70 MeV energy impinged on a thick (15 mg/cm^2) ^{45}Sc target. The beam energy was chosen to fulfill the Cline's safe Coulomb-excitation criterion [7]. The central European Array for Gamma Levels Evaluations (EAGLE) spectrometer [8] was used to detect γ rays depopulating the Coulomb-excited states in ^{45}Sc. The experiment was carried out without particle-γ coincidences. Further details can be found in Ref. [9].

A complementary measurement to study ^{45}Sc was performed at IUAC in New Delhi. A ^{32}S beam of 70 MeV energy was delivered by the 15UD tandem accelerator and impinged on a 1 mg/cm^2 ^{45}Sc target. The γ rays depopulating Coulomb-excited states in ^{45}Sc were detected by four clover detectors in coincidence with forward scattered ions. The scattered beam particles and the recoiling target nuclei were detected in the position sensitive Annular Parallel Plate Avalanche Counter (APPAC) [10]. Further experimental details can be found in Ref. [11].

3. Coulomb excitation data analysis

A set of reduced electromagnetic matrix elements was extracted from the measured γ-ray yields using the GOSIA code [7, 12, 13], which performs a multidimensional χ^2 minimization constrained by complementary spectroscopic information, such as branching ratios, E2/M1 mixing ratios, and lifetimes measured in previous experiments. Some results from the individual analyses of each experiment are reported in Refs. [9, 11].

In this contribution, we present the result of a combined analysis of both data sets collected at HIL and IUAC. The level scheme of ^{45}Sc considered in the current analysis is presented in Fig. 1. The observed γ-ray transitions are marked in blue/dark gray, red/light gray, and green/middle gray. The additional presented states include the so-called "buffer states" which were introduced in the analysis to ensure that virtual excitation and coupled-channel truncation effects are taken into account [12]. Three buffer states were included in ^{45}Sc: $7/2^+$ at 974 keV, $1/2^+$ at 939 keV, and $15/2^-$ at 2106 keV. Known branching ratios, E2/M1 mixing ratios, and lifetimes of excited states, listed in Refs. [9, 11], were included in the GOSIA analysis as additional information. These complementary experimental data increased the sensitivity of the analysis and were helpful in the evaluation of the influence of non-observed transitions on the measured excitation cross sections. When constructing the additional spectroscopic data set for ^{45}Sc, it was noticed that the half-lives of the $11/2^-$ state reported in the literature vary from 0.12(8) ps (from DSAM [14]), through 1.80(10) ps (from (γ, γ') [15]),

to 2.4(+10, −6) ps (from $(\alpha, p\gamma)$ [16]). Due to such large discrepancies, the lifetime value for this state was not included in the analysis as an additional spectroscopic data point to be fitted.

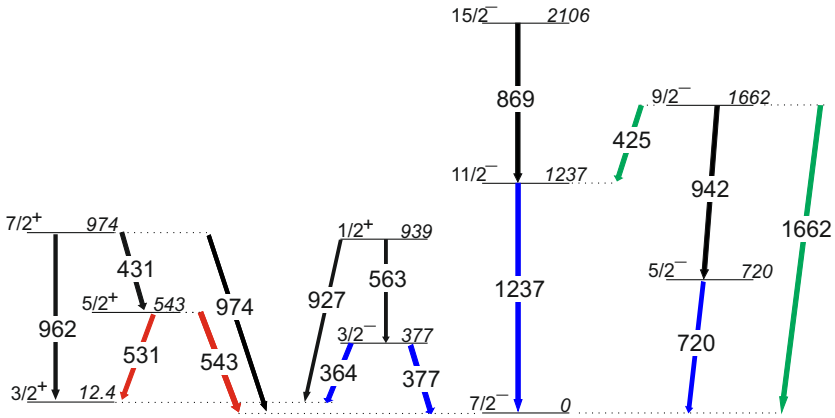

Fig. 1. (Color online) Low-lying level scheme of the ^{45}Sc isotope relevant for the present work. The energies are given in keV. Transitions marked in blue (dark gray) were observed in both experiments, transitions marked in green (middle gray) were observed only in the data from IUAC, while transitions marked in red (light gray) were observed only in the data collected at HIL. Transitions marked in black (*i.e.* those deexciting the $1/2^+$, $7/2^+$, and $15/2^-$ buffer states, and the 942 keV line) have not been observed in both experiments, however, the corresponding matrix elements were considered in the Coulomb-excitation data analysis with the GOSIA code.

To increase the sensitivity to the matrix elements relevant for the lifetime of the $11/2^-$ state at 1237 keV, the data collected at IUAC were subdivided into two sets based on the projectile scattering angle: one set having θ_{LAB} from 15° to 25° and a second set with θ_{LAB} from 25° to 45°. The experimental γ-ray yields were normalized to the intensity of the $3/2^- \rightarrow 7/2^-$ 377 keV transition, as the lifetime of the $3/2^-$ state and the branching ratio between the 377 keV and 364 keV transitions are known with a good precision.

A set of reduced matrix elements was extracted in the course of the present, combined analysis, which results in the reduced transition probability $B(\mathrm{E2}; 11/2^- \rightarrow 7/2^-) = 90 \pm 5\ e^2\mathrm{fm}^4$ and the lifetime for the $11/2^-$ state at 1237 keV, $\tau = .14 \pm 0.19$ ps ($T_{1/2} = .18 \pm 0.13$ ps). The diagonal matrix element of the $11/2^-$ state at 1237 keV as well as the feeding of this state via single- and double-step excitation (through the $9/2^-$ state at 1662 keV) were included in the analysis. The obtained value is closest to the outcome of the $(\alpha, p\gamma)$ reaction measurement [16].

Other reduced B(E2) transition probabilities extracted in the present analysis are presented in Table 1. Additionaly, an upper limit for the reduced excitation probability B(E3; $7/2^- \rightarrow 5/2^+$) equal to 1.7 W.u. has been determined for the first time from the HIL data (further details can be found in Ref. [9]).

4. Discussion

Large-scale shell-model calculations have been performed in the valence space comprising neutron and proton $s_{1/2}d_{3/2}$–$p_{3/2}f_{7/2}$ orbitals, known as the ZBM2 model space. In a first attempt, we employed the so-called ZBM2.renorm interaction [17, 18] available in the ANTOINE code package. However, this interaction has previously been shown to fail in reproducing, *e.g.*, the isotopic shifts in the Sc chain [5], and we also encountered diffculties to describe the evolution of the energy of the $3/2^+$ isomeric state along the Sc chain within this framework (see Fig. 2).

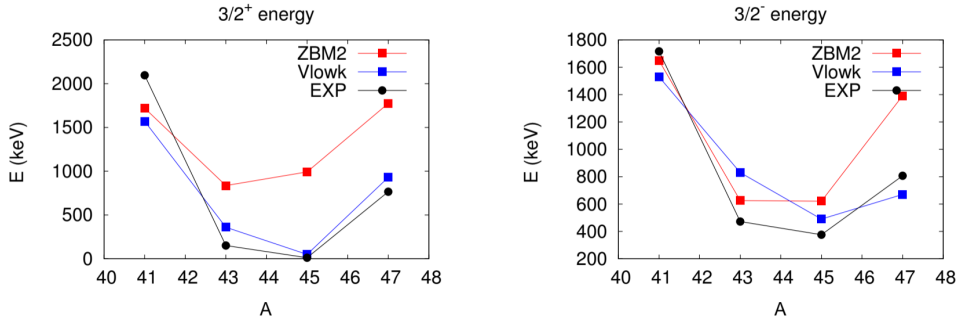

Fig. 2. Energy systematics of the low-lying $3/2^+$ and $3/2^-$ states in Sc isotopes with $A = 41$–47, compared with the large-scale shell-model calculations using the ZBM2 and the $V_{\mathrm{low}-k}$ interactions (see the text for details).

A second attempt was made to derive a new effective interaction for the full *sd*–*pf* space. The interaction is based on a realistic $V_{\mathrm{low}-k}$ potential, adapted to the model space using the many-body perturbation theory up to the 2$^{\mathrm{nd}}$ order. The single-particle energies in the core were adjusted to reproduce energies of one-hole states in ^{39}K and one-particle states in ^{41}Sc. In the first step, the calculations were restricted to the ZBM2 model space in which diagonalization of the Hamiltonian is achieved in the full configuration space. The evolution of excitation energies of the $3/2^-$ and $3/2^+$ states is shown in Fig. 2 for both interactions and the experimental data. The new interaction underestimates the energies in ^{41}Sc but the agreement improves with increasing neutron number. In particular, the excitation energy of the $3/2^+$ state in ^{45}Sc, the nucleus of our major interest, is calculated

to be 50 keV with the new effective interaction, while it is located at nearly 1 MeV with ZBM2. In addition, the evolution of the $3/2^-$ excitation energy improves for $V_{\mathrm{low}-k}$ with respect to ZBM2, resulting in a minimum at $A = 45$, in line with the experimental results.

The B(E2) values obtained in the present analysis, together with results of large-scale shell-model calculations with the ZBM2 and $V_{\mathrm{low}-k}$ interactions, are presented in Table 1. As we have shown in the beginning, the present calculations offer a major improvement concerning the location of the postive-parity band. Otherwise, both interactions predict similar B(E2) transition probabilities between the $3/2^-$ and the ground state. Major differences are however observed for the remaining states which seem more collective with the ZBM2 interaction. The experimental reduced transition probabilities for transitions depopulating the $5/2^-$ and $11/2^-$ states are in better agreement with the $V_{\mathrm{low}-k}$ interaction. As can be seen from Table 2, the quadrupole moment of the ground state is very close to the experimental value when using $V_{\mathrm{low}-k}$ but the one for the $3/2^+$ state is too low. Calculations permitting excitations from the sd to the full pf shell could result in a better agreement with the experimental data due to a larger collectivity. Development of interactions in such a large model space is in progress.

Table 1. Reduced B(E2) transition probabilities extracted from the present combined analysis of data collected at HIL and IUAC, compared with results of large-scale shell-model calculations with the ZBM2 and $V_{\mathrm{low}-k}$ interactions. Reduced B(E2) transition probabilities are in $e^2\mathrm{fm}^4$, while energies are in keV.

		GOSIA fit		ZBM2		$V_{\mathrm{low}-k}$	
J_i^π	J_f^π	Energy	B(E2)	Energy	B(E2)	Energy	B(E2)
$3/2^-$	$7/2^-_{\mathrm{gs}}$	377	142 ± 9	621	218	495	165
$5/2^-$	$7/2^-_{\mathrm{gs}}$	720	80 ± 5	457	278	1070	37
$9/2^-$	$7/2^-_{\mathrm{gs}}$	1662	66 ± 4	1808	39	1709	24.8
$9/2^-$	$11/2^-$	425	∼100 [1]	272	135	757	1.3
$11/2^-$	$7/2^-_{\mathrm{gs}}$	1237	90 ± 5	1536	189	952	57

[1] This value was included in the calculations and estimated based on literature data *i.e.* 1662/425 keV branching ratio and E2/M1 mixing ratio for the 425 keV line. The present analysis did not provide enough sensitivity to determine this value.

Table 2. Nuclear magnetic dipole moments μ_N and spectroscopic quadrupole moments Q of ^{45}Sc obtained with large-scale shell–model calculations using the ZBM2 and the V_{low-k} interactions in comparison to experimental data [5]. Magnetic moments are in μ_N, quadrupole moments in $e$fm^2.

J^π		Exp	ZBM2	V_{low-k}
$7/2^-_{gs}$	Q	−22.0(2)	−10.5	−23.3
	μ	4.756487(2)	4.499	4.238
$3/2^+$	Q	28(5)	16.2	19.6
	μ	0.360(11)	0.458	0.528

Alternatively, the collective character of the low-lying states in ^{45}Sc could be examined using mean-field methods [4]. The density-functional-theory approach, successfully used to study mirror energy differences in ^{45}Sc/^{45}Cr and ^{47}Ti/^{47}Mn [19, 20], was employed to characterize the low-lying states in ^{45}Sc including the $3/2^+$ isomer. The deformations associated with these excitations resulting from the calculation (for the g.s. $\beta = 0.16$, and for the $3/2^+$ isomer: $\beta = 0.27$ or $\beta = 0.28$, $\gamma = 4^\circ$ using Skyrme SLy4 and SVSO forces respectively), agree very well with the values extracted from experiments [4, 5]. On the other hand, the calculations fail to reproduce the very low excitation energy of the isomer in ^{45}Sc, which requires further investigation.

This work was supported by the National Science Centre (NCN), Poland under grant No. 2014/12/S/ST2/00483. The authors would like to thank the European Gamma-Ray Spectroscopy Pool GAMMAPOOL for the loan of the detectors for EAGLE. This work was partially supported by the U.S. Department of Energy, Office of Science, Office of Nuclear Physics, under contract number DE-AC02-06CH11357.

REFERENCES

[1] M.A. Bentley *et al.*, *Phys. Rev C* **73**, 024304 (2006).
[2] P. Bednarczyk *et al.*, *Eur. Phys. J. A* **2**, 157 (1998).
[3] J. Styczeń *et al.*, *Nucl. Phys. A* **262**, 317 (1976).
[4] P. Bednarczyk *et al.*, *Phys. Lett. B* **393**, 285 (1997).
[5] M. Avgoulea *et al.*, *J. Phys. G: Nucl. Part. Phys.* **38**, 025104 (2011).
[6] https://www.nndc.bnl.gov/ensdf/

[7] D. Cline, *Annu. Rev. Nucl. Part. Sci.* **36**, 683 (1986).
[8] J. Mierzejewski *et al.*, *Nucl. Instrum. Methods Phys. Res. A* **659**, 84 (2011).
[9] M. Matejska-Minda *et al.*, *Acta Phys. Pol. B* **49**, 567 (2018).
[10] A. Jhingan *et al.*, *Nucl. Instrum. Methods Phys. Res A* **922**, 209 (2019).
[11] M. Matejska-Minda *et al.*, *Acta Phys. Pol. B* **51**, 829 (2020).
[12] T. Czosnyka, D. Cline, C.Y. Wu, *Bull. Am. Phys. Soc.* **28**, 745 (1982).
[13] https://www.slcj.uw.edu.pl/en/gosia-code/
[14] M.K. Georgieva *et al.*, *Fiz. Elem. Chastits At. Yadra* **20**, 930 (1989).
[15] F.R. Metzger, *Phys. Rev. C* **12**, 312 (1975).
[16] J. Chevallier, B. Haas, N. Schulz, M. Toulemonde, *J. Phys. France* **37**, 303 (1976).
[17] E. Caurier, F. Nowacki, *Acta Phys. Pol. B* **38**, 1369 (2007).
[18] A. Poves *et al.*, *Eur. Phys. J. A* **20**, 119 (2003).
[19] S. Uthayakumaar *et al.*, *Phys. Rev. C* **106**, 024327 (2022).
[20] W. Satuła *et al.*, *Phys. Rev. C* **94**, 024306 (2016).